

FIG. 1. Energy spectrum of π^+ mesons at $18.0 \pm 0.9^\circ$. The peak occurs at 63.5 ± 0.3 Mev. The dotted curve includes a correction for nuclear absorption of mesons in slowing down. Based on 885 mesons.

using a "point" source of liquid hydrogen bombarded with nearly monoenergetic protons. Meson energies and the incident proton beam energy were determined by range in absorbers, using the tables of Aaron, *et al.*⁴ with slight corrections required by the absolute proton range-energy measurements of Segrè and Mather.⁵ The width of the observed peak (3.6 Mev) corresponds very nearly to that expected from a "line" broadened by the 0.5 percent⁶ inhomogeneity in the incident proton beam.

The peak meson energy of 63.5 ± 0.3 Mev and incident proton energy (342 ± 1 Mev) may be used to calculate a mass value for the π^+ meson of $279.0 \pm 1.5 m_e$. The integrated spectrum corrected for absorption is $(1.6^{+0.3}_{-0.2}) \times 10^{-28}$ cm²-steradian⁻¹, based on 885 mesons. The partial yields of the $p+n+\pi^+$ and $d+\pi^+$ reactions may be estimated by resolving the spectrum of Fig. 1 into a continuous distribution up to 60.0 Mev plus a line separated by 3.5 Mev. Since the energy resolution half-width is 1.8 Mev the position of the peak and the higher energy side of the curve are only slightly affected by the presence of the continuous spectrum. Good agreement with the experimental curve is obtained if the "line" contains 55 ± 10 percent of the mesons observed.

The preliminary measurement made at 30° using a line source geometry² has been repeated with the point source and better statistics (482 mesons). The integrated cross section at this angle, corrected for absorption, is $(5.8^{+1.2}_{-0.6}) \times 10^{-29}$ cm²-steradian⁻¹. However, the energy resolution of this spectrum, taken previous to the 18° run, is not sufficient to separate the partial reactions.

The cross section at $64^\circ \pm 8^\circ$ has also been determined, although the low yield and poor angular resolution make it difficult to

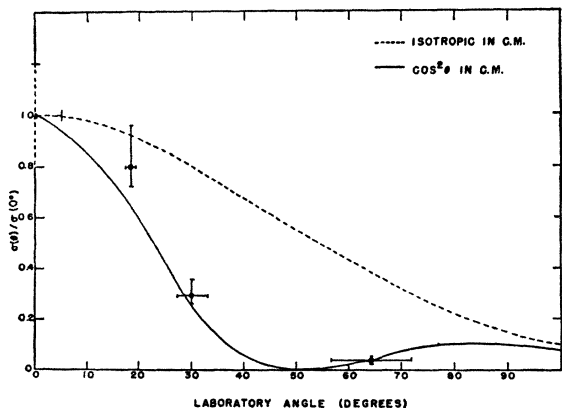


FIG. 2. Angular distribution of π^+ mesons in the laboratory system. The curves are calculated for the reaction $p+p \rightarrow d+\pi^+$ for 340-Mev protons.

obtain a significant energy spectrum. A value of $(7^{+4}_{-2}) \times 10^{-30}$ cm²-steradian⁻¹, based on 22 mesons, is calculated from the emulsion-target geometry and proton flux. An independent check of this value may be obtained by determining the yield of elastically scattered protons in the same emulsion. Using the known $p-p$ scattering cross section of 5.5 ± 1 mb/sterad⁷ (c.m. system) the meson/proton yield ratio gives a meson cross section of $11^{+6}_{-4} \times 10^{-30}$ cm²-steradian⁻¹.

These data, normalized to the 0° cross section measured by Cartwright, *et al.*,⁸ can be used to plot the angular distribution. The relative cross sections as a function of laboratory angle are plotted in Fig. 2. The angular distributions to be expected from pure isotropic or $\cos^2\theta$ production are also shown, for the case $p+p \rightarrow d+\pi^+$. A direct comparison of these curves to the experimental data assumes that most of the mesons are emitted with maximum energy at all angles. This assumption is supported by the energy spectra at 0° and 18° . Comparison of curves in Fig. 2 shows a strong preference for $\cos^2\theta$ emission.

If the angular distribution were strictly $\cos^2\theta$, the total cross section for π^+ production may be estimated to be $(2.3^{+0.4}_{-0.2}) \times 10^{-28}$ cm².

This work was sponsored by the Atomic Energy Commission.

- * Now at the California Institute of Technology, Pasadena, California.
¹ Cartwright, Richman, Whitehead, and Wilcox, Phys. Rev. **78**, 823 (1950); Phys. Rev. **81**, 652 (1951).
² V. Z. Peterson, Phys. Rev. **79**, 407 (1950); Peterson, Iloff, and Sherman, Phys. Rev. **81**, 647 (1951).
³ Crawford, Crowe, and Stevenson, Phys. Rev. **82**, 97 (1951).
⁴ Aaron, Hoffmann, and Williams, University of California Radiation Laboratory report UCRL-121 (2nd Rev.) (1949) (unpublished).
⁵ R. L. Mather and E. Segrè, Phys. Rev. **84**, 191 (1951).
⁶ C. J. Bakker and E. Segrè, Phys. Rev. **81**, 489 (1951).
⁷ O. Chamberlain and C. Wiegand, Phys. Rev. **79**, 81 (1950).
⁸ F. Cartwright (private communication).

Note on the Compound Dirac Equation*

D. C. PEASLEE†

Washington University, St. Louis, Missouri

(Received August 13, 1951)

SOME systematic remarks are made on a recent proposal¹ for combining Dirac equations with positive and negative times. The indices $j, k=1$ to 3; $\mu, \nu=1$ to 4; $A, B=1$ to 6.

Consider a Dirac equation and its time reverse:

$$\begin{aligned} (\partial_j \gamma_j + \partial_4 \gamma_4 + \kappa) \psi &= 0 \\ (\partial_j \gamma_j - \partial_4 \gamma_4 + \kappa) \psi' &= 0, \quad \psi' = i \gamma_{123} \psi. \end{aligned} \quad (1)$$

These two 4-rowed equations can be simply superposed to give an 8-rowed equation

$$(\partial_\mu \eta_\mu + \kappa) \varphi = 0, \quad (2)$$

where, if $\sigma_x, \sigma_y, \sigma_z$ are 2×2 Pauli matrices and $\mathbf{1}$ the corresponding unit matrix,

$$\eta_j = \mathbf{1} \gamma_j, \quad \eta_4, \eta_5, \eta_6 = \sigma_x \gamma_4, \sigma_y \gamma_4, \sigma_z \gamma_4. \quad (3)$$

The η_A are all hermitian and satisfy the equation

$$\eta_{AB} + \eta_{BA} = 2\delta_{AB}. \quad (4)$$

The invariance of (2) to a Lorentz transformation $x'_\mu = a_{\mu\nu} x_\nu$ depends in the usual way on the existence of a transformation matrix S such that

$$\eta_\mu a_{\mu\nu} = S^{-1} \eta_\nu S. \quad (5)$$

In terms of the η_A , there are four quantities that commute with all η_μ and hence transform as scalars under (5); namely,

$$1, i\eta_{56}, \eta_{12345}, \eta_{12346} = 1, \eta_7, \eta_8, i\eta_{78} = \{Y\}. \quad (6)$$

Thus any transformation operator can be generalized from the 4-rowed to the 8-rowed representation by $S(\gamma) \rightarrow S(\eta)Y$. This type

of generalization also holds for operators Q of which the expectation value is to be taken, $\psi Q(\gamma)\psi \rightarrow \bar{\varphi} Q(\eta) Y' \varphi$, where Q is one of the five covariant forms familiar in β -decay. It will be seen below that the set Y' includes only half the members of Y .

The equation adjoint to (2) is

$$\partial_\mu \bar{\varphi} \eta_\mu - \kappa \bar{\varphi} = 0, \quad \bar{\varphi} = \varphi^{T*} \eta_4. \quad (7)$$

where the superscript T denotes the transpose. The above generalization also applies here, and $\bar{\varphi} Y$ is a perfectly good adjoint solution. But since $\bar{\varphi}$ is of interest only in bilinear forms $\bar{\varphi} Q Y' \varphi$, and $Y Y' \rightarrow Y'$, it is sufficient to select a unique adjoint function as in (7), provided that Y' ranges over all possible values.

The possible operators Y' are seen by characterizing them in terms of the representation $\varphi = \begin{pmatrix} \psi \\ \psi' \end{pmatrix}$; then $Y' \varphi = \begin{pmatrix} y\psi \\ y'\psi' \end{pmatrix}$, where for η_7 , $y = -y' = 1$, and for η_8 , $y = y' = -1$. Consider the bilinear form $\bar{\varphi} Q Y' \varphi = y \bar{\psi} Q \psi \pm y' \bar{\psi}' Q \psi'$, where the \pm is as Q does or does not contain the index 4 and comes from the ± 1 eigenvalues of σ_4 in $\eta_4 = \sigma_4 \gamma_4$. Then by (1) $\bar{\psi}' Q \psi' = \pm \bar{\psi} Q \psi$ according as Q does or does not contain γ_4 on account of the commutation properties with γ_{123} . Thus, $\bar{\varphi} Q Y' \varphi = (y+y') \bar{\psi} Q \psi \equiv 0$ if Y' contains η_7 , and hence

$$\{Y'\} = 1, \eta_8. \quad (6a)$$

Note that the set (6a) depends on the choice (7) for the adjoint function $\bar{\varphi}$; if the adjoint were taken as $\bar{\varphi} Y_a$, the general condition would be that $\{Y' Y_a\} = 1, \eta_8$.

Judicious combination of Y and Y' permits some flexibility in the transformation properties of bilinear forms. Let $\bar{\varphi} Q Y' \varphi$ be transformed under $S Y$; then since η_7, η_8 anticommute, the algebraic sign under transformation is the same as for the 4-rowed case if $Y' = 1$ or if $Y' = \eta_8, Y = 1, \eta_8$, but is reversed if $Y' = \eta_8, Y = \eta_7, i\eta_8$. This applies, for instance, to the behavior of $(\bar{\varphi} \varphi)$ under time reversal. It also applies to the five β -decay invariants under charge and complex conjugation, so that the groupings (*SAP*) and (*TV*) found in the 4-rowed representation² may be arbitrarily altered. This arbitrariness fails only in the case of the energy and charge densities, which are presumably derivable from a single lagrangian and hence must transform with opposite sign under time reversal in any case.

It is curious but of little apparent use that the η_A are the matrices of a six-dimensional Dirac equation. The four choices of Y correspond to the four combinations of reversal and non-reversal of the unphysical coordinates x_5 and x_6 . This aspect also provides a direct proof that the η_A are irreducible, for they build the components of antisymmetric tensors in six dimensions of the 0, 1, 2, 3, 4, 5, 6th rank with $(1+6+15+20+15+6+1) = 8 \times 8$ independent elements. All representations are thus equivalent to (3).

* Assisted by the joint program of the ONR and AEC.
 † Now at Columbia University, New York.
 ‡ L. Biedenharn, Phys. Rev. **82**, 100 (1951).
 § S. R. de Groot and H. A. Tolhoek, Physica **16**, 456 (1950).

Low Frequency Dispersion in Ni- and Co-Ferrites

KAN-ICHI KAMIYOSHI

The Research Institute for Scientific Measurements, Sendai, Japan

(Received August 31, 1951)

GALT, Matthias, and Remeika¹ observed the low frequency dispersion of the magnetic permeability in Ni-ferrite, and recently Koops² found the low frequency dispersion of the dielectric constant in NiZn-ferrite. The present paper describes the electric low frequency dispersion in Ni- and Co-ferrites.

Real and imaginary dielectric constants, ϵ' and ϵ'' , and the dielectric loss factor, $\tan \delta$, were measured in vacuum by a Schering bridge with a sample which is 17 mm in diameter and 5 mm in thickness. The sample was prepared by sintering at 1200°C for 3 hours and was rapidly cooled in air from 1200°C. Figure 1 shows the curves of $\tan \delta$ versus temperature for different frequencies.

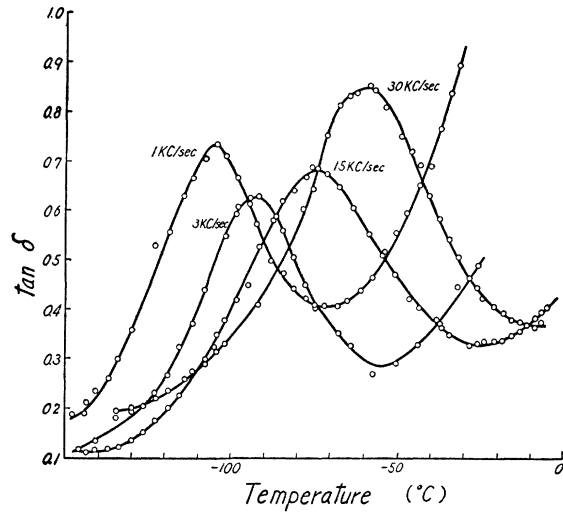


FIG. 1. Curves of $\tan \delta$ with varying temperature for Ni-ferrite.

Breckenridge³ considered the relaxation process for the low frequency dispersion in ionic crystals and gave the following equation:

$$\tau = \tau_0 e^{E/kT}, \quad (1)$$

where τ_0 and τ are the time constants for the natural vibration and the orientation process, respectively, and E the activation energy. Assuming this equation to hold for the ferrite and taking $\tau = [(\epsilon_0 + 2)/(\epsilon_1 + 2)](\epsilon_1/\epsilon_0)^{1/2}(1/\omega)$, where ϵ_1 and ϵ_0 are the static and very high frequency dielectric constants,⁴ respectively, we obtain a linear relation of $\log(1/\omega)$ against $1/T$ for each peak point of $\tan \delta$ for various frequencies; this is shown in Fig. 2. From the linear relation in this figure, we obtain $E = 0.23$ ev. It is noticeable that this activation energy is equal to the energy, $E_{\text{cond}} = 0.23$ ev, obtained from the electrical conductivity measurements which were made on the same sample. Therefore, it is expected that the origin of the anomalous dispersion in ferrites may be a similar mechanism to that of the electrical conductivity.

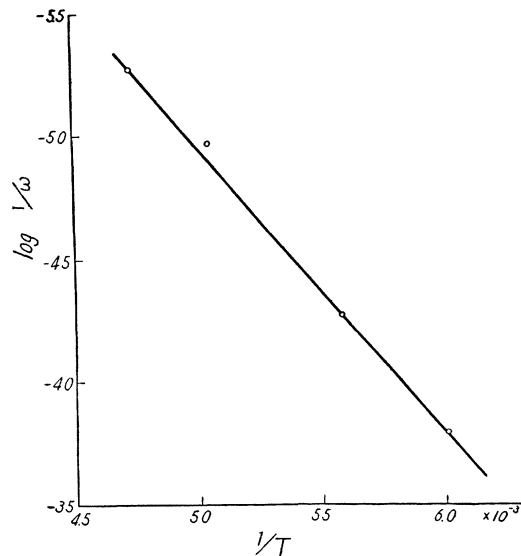


FIG. 2. Relation between $\log(1/\omega)$ and $1/T$ for Ni-ferrite.